UTILIZING NDVI AND NDII INDICES FOR COMPREHENSIVE CROP MONITORING AND IRRIGATION PERFORMANCE ASSESSMENT

Williams A. James[1], Ophaphaibun Chainarong[2], Maekan Ekkarin[3], Kowsuvon Noppadon[4], Maneephai Satit[5], Suiadee Watchara[6], Prechawit Chaiwat[7] and Sriwongsitanon Nutchanart*[8]

ABSTRACT

Remote sensing is vital for precision agriculture in Thailand, where the Royal Irrigation Department (RID) manages water for 3.5 million hectares. Wet season crops rely mainly on rainfall, while dry season farming depends on reservoirs with about 76,000 MCM capacity - only 30-60% of which is available during dry periods. Real-time crop monitoring is crucial for efficient water use and productivity. This study used MODIS imagery (2010–2024) to derive annual NDVI and NDII values, classifying land into 30 categories via K-Means across four irrigation projects. Average irrigated areas ranged from 17,071 to 49,190 ha based on RID data. Classification accuracy was enhanced with a refinement method from Remote Sensing Research Centre for Water Resources Management (SENSWAT). A comparative analysis of land use classification accuracy (2010–2024) across the projects assessed NDVI and NDII using Overall Accuracy (OA) and Kappa Coefficient (K), before and after enhancement. Nongwai and Lampao, with high initial accuracy (OA > 98%, K ~0.78-0.80), showed slight improvements (up to 99% OA, K ~0.92). Kraseaw improved moderately (83% to 86% OA; K ~0.63 to 0.69), while Northern Rangsit, with the lowest initial accuracy (OA ~71-73%, K ~0.39-0.44), improved significantly to 78.8% for OA and 0.56 for K. These results highlight the enhancement procedure's effectiveness, especially in low-accuracy areas. Crop area estimates from NDII and NDVI showed strong agreement (R^2 = 0.90-1.00; RMSE = 1.42-6.89%) across the four projects. NDII generally correlated slightly better with official RID data than NDVI. The findings also reveal discrepancies in official records and underscore the importance of real-time satellite-based monitoring for supporting data-driven agricultural management.

From 2013 to 2024, correlations between NDVI and NDII provided valuable insights into the relationship between crop growth and water availability across four major irrigation projects in Thailand. Strong correlations were observed in areas with controlled irrigation and variable water supply - Kraseaw showed consistent year-round correlations (r ~0.68-0.70), while Nongwai and Lampao exhibited high correlations during the dry season (r ~0.70-0.73). In contrast, correlations during the wet season were lower (r ~0.47), likely due to rainfall-driven water inputs. Northern Rangsit consistently displayed weak correlations (r ~0.25 for wet paddy fields, 0.43 for dry paddy fields, and 0.27 for orchards), reflecting stable and abundant water availability that limits NDII's sensitivity to moisture variation. Together, NDVI and NDII serve as effective tools for real-time crop monitoring and offer practical indicators of irrigation efficiency. These findings underscore the strong connection between crop growth and water dynamics, driven by both rainfall and irrigation practices. The Kraseaw project, in particular, exemplifies efficient water management by aligning crop growth with available water resources. Understanding such relationships is crucial for optimizing irrigation strategies, especially in water-scarce regions, enabling informed decision-making that promotes sustainable agriculture and improved crop productivity.

Keywords: Crop monitoring, Remote sensing, Normalized Difference Vegetation Index (NDVI), Normalized Difference Infrared Index (NDII), Land use classification.

[1] Researcher, Remote Sensing Research Centre for Water Resources Management (SENSWAT), Water Resources Engineering, Faculty of Engineering, Kasetsart University, Bangkok, Thailand; E-mail: james.kus41@gmail.com

[2] Researcher, Remote Sensing Research Centre for Water Resources Management (SENSWAT), Water Resources Engineering, Faculty of Engineering, Kasetsart University, Bangkok, Thailand; E-mail: chainarong.opb@gmail.com

[3] Researcher, Remote Sensing Research Centre for Water Resources Management (SENSWAT), Water Resources Engineering, Faculty of Engineering, Kasetsart University, Bangkok, Thailand; E-mail: m.ekkarin83@gmail.com

[4] Senior Expert on Irrigation Engineering, ICID, THAICID, Royal Irrigation Department; E-mail: princethai@gmail.com

[5] Chairman of Working Group on Technical Activity Thai National Committee on Irrigation and Drainage (THAICID), ICID, THAICID, Royal Irrigation Department; E-mail: nalayer02@gmail.com

[6] Vice President, ICID Vice President of THAICID, Thai National Committee on Irrigation and Drainage (THAICID) Executive Advisor on Irrigation Engineering (Operation and Maintenance), ICID, THAICID, Royal Irrigation Department; E-mail: watchara04_rid@icloud.com

[7] Honourable Vice President of ICID, ICID, THAICID, Royal Irrigation Department; E-mail: chaiwat.prechawit@gmail.com

[8] *Corresponding author, Head of Remote Sensing Research Centre for Water Resources Management, Remote Sensing Research Centre for Water Resources Management (SENSWAT), Water Resources Engineering, Faculty of Engineering, Kasetsart University, Bangkok, Thailand; E-mail: fengnns@ku.ac.th

1. Introduction

Remote sensing has emerged as a vital tool for monitoring crop production and land use, providing a cost-effective, consistent, and timely alternative to traditional field-based methods. Satellite-based Earth observation enables large-scale, repeatable assessments of cultivated land and crop health, overcoming the limitations of manual inspections (Duveiller, 2010; Atzberger, 2013; Thenkabail et al., 2012; Dorj et al., 2017). This spatially explicit approach enhances agricultural monitoring and supports food security planning amid climate uncertainties (Bargoti & Underwood, 2017; Lobell et al., 2015). Moreover, remote sensing allows frequent data collection for time-series analysis (Rogan & Chen, 2004), offers multi-scale and multi-resolution applications (Pickering et al., 2021), enables rapid remote processing (Sishodia et al., 2020), and facilitates early detection of plant stress through electromagnetic data.

Vegetation indices (VIs) are essential tools widely used in agricultural remote sensing to assess vegetation health, biomass, and canopy characteristics. Among these, the Normalized Difference Vegetation Index (NDVI), introduced by Rouse et al. (1973), is one of the most extensively applied. NDVI exploits the contrast in reflectance between red (absorbed by chlorophyll) and near-infrared (reflected by healthy vegetation) wavelengths to quantify vegetation vigor (Tucker, 1979). This index has been used in numerous agricultural applications, including crop type classification (Wardlow & Egbert, 2008), growth stage monitoring (Zhang et al., 2003), drought assessment (Peters et al., 2002), and yield prediction (Basso et al., 2006). Additionally, NDVI is valuable for detecting plant stress due to pests, nutrient deficiencies, or water scarcity, and plays a key role in supporting precision agriculture by enabling site-specific management decisions (Mulla, 2013; Hatfield & Prueger, 2010).

The Normalized Difference Infrared Index (NDII) is a valuable vegetation index used to assess plant water content and detect moisture stress by analyzing the reflectance differences between near-infrared (NIR) and shortwave infrared (SWIR) bands (Hardisky et al., 1983; Gao, 1996). NDII is particularly effective for identifying early signs of water stress before visual symptoms appear, making it a critical tool in crop monitoring. Its applications include detecting drought-affected areas, supporting irrigation planning, and enhancing drought assessment when combined with NDVI (Serrano et al., 2000; Jackson et al., 2004; Delbart et al., 2005). Additionally, NDII contributes to crop yield prediction models for crops such as maize and wheat, aids in tracking phenological stages related to soil moisture and supports precision agriculture by enabling site-specific water management (Claverie et al., 2018; Liu et al., 2017).

This study aims to investigate the relationship between the Normalized Difference Vegetation Index (NDVI) and the Normalized Difference Infrared Index (NDII) to enhance land use classification and crop monitoring in four major irrigation projects in Thailand, covering nearly 150,000 hectares. By analyzing time-series satellite data from 2013 to 2024, the study explores seasonal land use dynamics and examines the correlation between vegetation growth and moisture availability. The ultimate goal is to assess the potential of the NDVI–NDII relationship as a reliable indicator of irrigation performance.

2. Study area

Thailand has approximately 5 million hectares of irrigated land managed by the Royal Irrigation Department (RID), distributed across 17 regional irrigation offices nationwide, as shown in Figure 1. This study focuses on four major irrigation projects: Kraseaw, Nong Wai, Lampao, and the Northern Rangsit Operation and Maintenance Projects. Together, these projects encompass a total area of 167,111 hectares, with individual areas of 19,082, 46,281, 53,419, and 48,329 hectares, respectively, as detailed in Table 1 and shown in Figure 1.

The irrigated areas in the four studied projects are categorized into six primary land use classes based on data from the Land Development Department (2019–2021). The dominant land use is paddy fields, accounting for 74.91% of the total area, followed by perennial and orchard crops (9.01%), urban areas (4.46%), field crops (5.68%), water bodies (5.83%), and forest (0.11%).

3. Methodology

3.1 Data acquisition and preprocessing

The primary data used for land use identification within the four irrigation projects are NDVI and NDII time series from 2013 to 2024. The resulting land use classifications were compared with land use maps from the Land Development Department (LDD) and cropping area records reported by the Royal Irrigation Department (RID). Details of the data acquisition and preprocessing steps are described in the following sections.

Table 1. Land use classification within four irrigation projects based on LDD data

Description	Irrigation projects area									
	Kraseaw		Nongwai		Lampao		Northern Rangsit		Total	
	ha	%	ha	%	ha	%	ha	%	ha	%
Paddy fields	12,567	65.86	39,443	85.22	48,999	91.73	24,172	50.02	125,181	74.91
Field crops	5,629	29.50	2,148	4.64	447	0.84	1,271	2.63	9,495	5.68
Perennial and orchard crops	100	0.52	993	2.15	262	0.49	13,707	28.36	15,062	9.01
Forest	-	-	177	0.38	-	-	-	-	177	0.11
Urban areas	785	4.12	1,594	3.44	1,717	3.21	3,350	6.93	7,447	4.46
Water bodies	-	-	1,925	4.16	1,994	3.73	5,829	12.06	9,749	5.83
Total	19,082	100.00	46,281	100.00	53,419	100.00	48,329	100.00	167,111	100.00

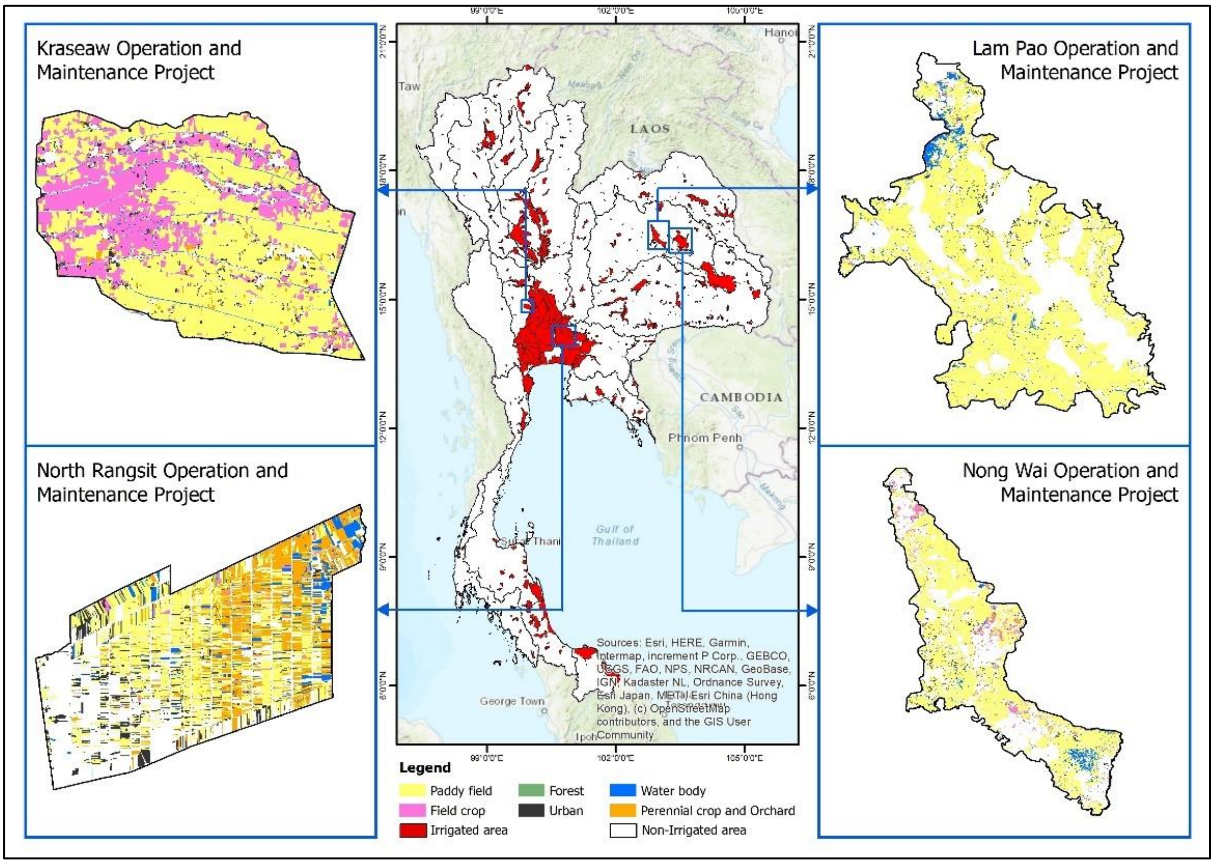

Figure 1. Irrigation projects in study area including (a) Nongwai, (b) Lampao, (c) Kraseaw and (d) Northern Rangsit

3.1.1 Normalized Difference Vegetation Index (NDVI)

The Normalized Difference Vegetation Index (NDVI) is one of the most commonly used remote sensing indices for evaluating vegetation health (Rouse et al., 1979). Because it is sensitive to chlorophyll, NDVI is particularly effective for tracking seasonal changes in vegetation greenness (Wang and Tenhunen, 2004). NDVI is calculated using the difference between red (RED) and near-infrared (NIR) reflectance, as shown in Eq. (1). The resulting values range from -1 to 1. Higher NDVI values (closer to 1) indicate healthy, dense vegetation. Values near zero usually represent bare soil or sparsely vegetated land, while negative values are typically associated with surfaces like water, snow, or clouds (Aburas et al., 2015). In addition to monitoring vegetation health, NDVI is widely used in applications such as land use and land cover classification (Eisfelder et al., 2023; Liu et al., 2022; Aburas et al., 2015; Ali et al., 2013).

In this study, multi-temporal NDVI imagery was obtained from the MODIS sensor aboard NASA's Terra (AM-1) satellite. Specifically, the MOD13Q1 Version 6 product was used, which provides 16-day composite vegetation indices at a spatial resolution of 250 meters. This product has been atmospherically corrected for Rayleigh scattering, ozone absorption, and aerosol effects to enhance the accuracy of surface reflectance values. The dataset is publicly available through the USGS Earthdata portal at: https://e4ftl01.cr.usgs.gov/MOLT/MOD13Q1.006 (Didan et al., 2015).

$$NDVI = \frac{NIR-RED}{NIR+RED} \quad (1)$$

3.1.2 Normalized Difference Infrared Index (NDII)

The Normalized Difference Infrared Index (NDII), first introduced by Hardisky et al. (1983), is widely used to assess vegetation water content. It is a valuable tool in a range of applications, including agricultural crop monitoring, forest canopy analysis, and the detection of plant water stress (Steele-Dunne et al., 2012). NDII is calculated using surface reflectance measurements from the near-infrared (NIR) and shortwave-infrared (SWIR) spectral bands, as shown in Equation (2). These reflectance values are available from the MODIS MOD09A1 product, which provides imagery at a spatial resolution of 500 metres and an 8-day temporal interval, with a data latency of approximately two weeks (Vermote et al., 2015).

$$NDII = \frac{NIR-SWIR}{NIR+SWIR} \quad (2)$$

NDII values range from -1 to +1, with values greater than 0.4 indicating healthy, water-rich vegetation. Values between 0.2 and 0.4 suggest moderate moisture levels, often associated with less dense or moderately stressed vegetation. Values ranging from 0 to 0.2 indicate low water content, typically reflecting dry or water-stressed vegetation. Values below 0 generally correspond to non-vegetated surfaces, such as bare soil, water bodies, or urban areas, and may also indicate areas of severe vegetation stress (Gonsamo et al., 2012).

3.2 Land use classification using NDVI and NDII

K-means clustering (Sharma et al., 2019; Lloyd, 1982), an unsupervised classification method, was applied to NDVI and NDII data for land use classification across four irrigation projects. The annual NDVI and NDII datasets, containing 46 and 236 images per year, respectively, were consolidated into a single dataset (46 × number of pixels and 23 × number of pixels). Subsequently, the NDVI and NDII data were classified into land use categories using the K-means clustering approach. Non-agricultural areas—including water bodies, urban zones, and forests—were excluded from the analysis to focus exclusively on cropping areas.

K-means clustering is a popular unsupervised learning technique used to group data into k clusters by minimizing the variation within each cluster (Arthur & Vassilvitskii, 2007). The process starts with selecting initial centroids, after which each data point is assigned to the nearest centroid using Euclidean distance. These centroids are then recalculated as the average position of the points in their respective clusters. This cycle of assignment and updating continues until the centroids no longer move significantly or a maximum number of iterations is reached (Lloyd, 1982). Known for its simplicity and computational efficiency, K-means is frequently applied to large, high-dimensional datasets, particularly in remote sensing, where it's commonly used for tasks like land use and land cover classification (Zhao et al., 2020; Sharma et al., 2021).

3.3 Accuracy assessment of land use classification using NDVI and NDII

Land use classifications derived from NDVI and NDII for the four irrigation projects were evaluated against land use data from the LDD using Overall Accuracy (OA), as defined in Equation (3) (Olofsson et al., 2013), and the Kappa Coefficient (K), as shown in Equation (4) (Lu & Weng, 2007). Some discrepancies between the datasets can be attributed to the static nature of the LDD database, which is updated only every 2–3 years, whereas NDVI- and NDII-based classifications capture annual variations. To further validate the classification accuracy, comparisons were also made using field data collected by the RID.

$$\text{Overall Accuracy} = \frac{\sum_{i=1}^{r} x_{ii}}{x} \quad (3)$$

where x_{ii} is the diagonal elements in the error matrix, x is the total number of samples in error matrix.

$$\text{Kappa Coefficient (K)} = \frac{n\sum_{i=1}^{r} x_{ii} - \sum_{i=1}^{r} x_{i+}x_{+i}}{n^2 - \sum_{i=1}^{r} x_{i+}x_{+i}} \quad (4)$$

where r is the number rows in the matrix, x_{ii} is the number of observations in row i and column i, x_{i+} and x_{+i} are marginal totals for row i and column i respectively and n is the total number of observations (pixels).

3.4 Enhancing the accuracy of land use classification using NDVI and NDII

Due to the static nature of the LDD database, discrepancies were found when comparing land use classifications derived from NDVI and NDII indices. To improve classification accuracy, this study adopted a methodology developed by the Remote Sensing Research Centre for Water Resources Management (SENSWAT), Faculty of Engineering, Kasetsart University. This approach refines NDVI- and NDII-based land use classifications by comparing them with LDD data. It identifies correctly matched pixels (Intersect), calculates the RMSE for mismatched pixels (Non-Intersect), and reassigns those classified as "Non-Intersect but Correct" to their appropriate land use category—ultimately enhancing the overall accuracy of the classification.

3.5 Relationship between NDVI vs NDII

NDVI and NDII are key remote sensing indices which can be used for real-time crop monitoring, supporting improved water allocation and agricultural productivity. NDVI measures vegetation health and growth by detecting chlorophyll levels, while NDII assesses plant water content and moisture stress. Their combined use provides insights into irrigation effectiveness, with a higher correlation between the two indicating better alignment between water application and crop growth. In this study, the correlation coefficient was used to assess this relationship during the wet and dry seasons for each crop across four major irrigation projects.

4. Results and Discussion

4.1 Crop classification from K-Means classification

K-means clustering was applied to annual NDVI and NDII datasets from 2013 to 2024 across four irrigation projects to classify land use. To further enhance classification accuracy, an improvement procedure was subsequently implemented. Figures 2 to 5 present examples of the land use classification process using NDII data for the Kraseaw, Nong Wai, Lampao, and Northern Rangsit Operation and Maintenance Projects. Each figure comprises three components, as described below:

(a) Land use classification map showing 30 classes generated using K-means clustering.

NDII data for each water year were classified into 30 distinct classes using K-means clustering. For each class, box plots display the NDII values and the number of pixels assigned to that class. Based on the NDII signature of each pixel (see first figure in panel (b)), green represents paddy fields, while purple represents field crops.

(b) Comparison of four land use maps:

1. Land use defined by LDD.

Green pixels represent paddy fields, and purple pixels represent field crops, based on the class signatures of the 30 clusters shown in panel (a) and described above.

2. Thirty land use classes classified using K-means.

3. Three generalized land use classes derived by aligning LDD categories with the K-means classification results.

These three classes include: one-season paddy fields, two-season paddy fields, and field crops. The example shown is from Figure 2; the specific classification results for Figures 3 to 5 may vary accordingly.

4. Refined three-class land use map produced using the accuracy enhancement procedure.

(c) Box plots showing NDII and NDVI signatures for each crop type.

These plots represent the final NDII and NDVI signatures for each crop type, based on individual pixel classifications shown in panel (b4).

Figure 6 presents a comparison of the original and enhanced Overall Accuracy (OA) and Kappa Coefficient (K) for land use classification from 2010 to 2024 across four irrigation projects, using NDVI and NDII indices. In the Kraseaw Irrigation Project, the original OA and K values were approximately 83% and 0.63, respectively. After applying the enhancement method, modest improvements were observed, with OA rising to about 86% and K to 0.69 (Figure 6a). For the Nongwai and Lampao projects, both exhibited high initial classification accuracy (OA ~98%, K ~0.78–0.79). Post-enhancement values showed only slight increases, reaching up to 99% OA and K values of 0.88 and 0.92, respectively, due to their already strong baselines (Figures 6b and 6c). In contrast, the Northern Rangsit Irrigation Project initially had the lowest accuracy (OA ~71–73%, K ~0.39–0.44). Following enhancement, OA improved to 78.8% and K to 0.56, indicating that the refinement process was particularly effective in lower-performing areas (Figure 6d).

4.2 Comparison of crop areas classified by NDII and NDVI with RID data

Land use classifications derived from NDII and NDVI were analyzed for the period from 2010 to 2024 and compared with irrigated area data reported by the Royal Irrigation Department (RID) from 2013 to 2024. It is important to note that the spatial resolutions of the two indices differ: NDII has a coarser resolution of 500 meters per pixel, while NDVI offers a finer resolution of 250 meters. To ensure meaningful comparison, crop area estimates from NDII were adjusted to match the spatial scale of NDVI.

The NDVI-based crop area estimates were 18,197 km² for the Kraseaw Project, 41,591 km² for the Nong Wai Project, and 49,808 km² for the Lampao Operation and Maintenance Project. In contrast, the irrigated areas reported by the Royal Irrigation Department (RID) for these regions were 17,071 km², 49,190 km², and 42,360 km², respectively. Due to discrepancies between the crop area estimates derived from both NDVI and NDII and the figures reported by RID, further adjustments were made to harmonize all datasets with the RID-reported values.

For the Northern Rangsit Irrigation Project, the irrigated area reported by the RID showed considerable variability, ranging from 21,423 km² in 2021 to 42,360 km² in 2024, with an average of 31,572 km² over the observed period. In contrast, the NDVI-based estimate of crop area for the same region was 39,150 km². The substantial fluctuation in RID-reported figures reduces their reliability for direct comparison with land use classifications derived from NDVI and NDII indices. As a result, a comparison between crop areas based on NDVI and NDII and those reported by the RID was not conducted.

Figure 7 compares crop areas classified using NDVI and NDII indices with irrigated areas reported by the RID across four major irrigation projects from 2010 to 2024. The Kraseaw project includes wet and dry season paddy fields and field crops, while the Nongwai and Lampao projects mainly involve paddy cultivation. The Northern Rangsit project covers paddy fields and orchard areas.

The cropping areas identified using NDII and NDVI were compared with each other and also against data reported by the RID. The results showed that the crop areas classified using NDII and NDVI across all seasons for the Kraseaw, Lampao, Nongwai, and Northern Rangsit projects were highly consistent with one another, with coefficients of determination (R^2) of 1.00, 0.99, 0.92, and 0.95, respectively. The relative Root Mean Square Error (RMSE) values between NDII and NDVI were low, at 2.00%, 1.42%, 2.15%, and 6.89%, respectively, indicating strong agreement between the two indices.

In comparison, the correlation between NDII-derived crop areas and RID-reported data yielded R^2 values of 0.97, 0.74, and 0.70 for Kraseaw, Lampao, and Nongwai, respectively. For NDVI versus RID data, the corresponding R^2 values were slightly lower at 0.97, 0.72, and 0.61. The relative RMSE values for NDII compared to RID were 7.68%, 7.67%, and 3.81%, respectively, while for NDVI they were 8.34%, 7.18%, and 4.54%.

Overall, NDII and NDVI provide similar crop area estimates, with NDII slightly better aligned to RID data. Differences between satellite estimates and RID records likely reflect variability in official reporting or classification challenges in certain areas.

4.3 Relationship between pixel-based NDII and NDVI

Figure 8 illustrates the correlation coefficients (r) between NDII and NDVI for various crop types across four irrigation projects from 2013 to 2024, providing insights into the relationship between plant water content and crop growth. In the Kraseaw project, correlations are strong and consistent across crop types, with average values around 0.68–0.70 for both wet and dry season paddy fields and 0.67 for field crops. This reflects well-defined growing periods supported by effective irrigation management.

At Nongwai and Lampao, wet season paddy fields show moderate correlations (avg. ~0.47), likely influenced by variable rainfall, while dry season paddy fields exhibit stronger correlations (avg. ~0.71–0.73), indicating more stable water availability from irrigation during the dry season. In contrast, Northern Rangsit displays generally weak correlations across all land uses—wet season paddy (avg. 0.25), dry season paddy (avg. 0.43), and orchards (avg. 0.27). This suggests that consistently abundant water from intensive irrigation and groundwater reduces NDII sensitivity to moisture variation, weakening its correlation with NDVI. Overall, these results highlight that stable irrigation during the dry season strengthens the link between vegetation growth and water content, while variability in rainfall and consistently high-water availability affect correlation strength differently across projects.

5. Conclusions

This study highlights the effectiveness of MODIS-derived NDVI and NDII for long-term crop monitoring and irrigation assessment across four major irrigation projects in Thailand. Using K-Means clustering and refinement by SENSWAT, land use classification accuracy significantly improved, especially in low-performing areas like Northern Rangsit. Crop area estimates from NDVI and NDII closely matched official RID data (R^2 = 0.90–1.00), with NDII showing slightly better alignment.

Correlation analysis (2013–2024) revealed strong NDVI–NDII relationships in areas with active irrigation and variable water supply—particularly in Kraseaw and during the dry season in Nongwai and Lampao—while weaker correlations in Northern Rangsit reflected stable water conditions. Together, NDVI and NDII provide valuable indicators of irrigation efficiency and crop–water dynamics. The Kraseaw project stands out for its effective water management, underscoring the value of real-time satellite monitoring for optimizing irrigation, enhancing productivity, and promoting sustainable agriculture in water-scarce regions.

REFERENCES

Aburas, M. M., Abdullah, S. H., Ramli, M. F., Ash'aari, Z. H., 2015. Measuring land cover change in Seremban, Malaysia using NDVI index. Procedia Environmental Sciences, 30, 238-243.

Ali, A., De Bie, C., Skidmore, A. K., Scarrott, R. G., Hamad, A., Venus, V., & Lymberakis, P. (2013). Mapping land cover gradients through analysis of hyper-temporal NDVI imagery. International Journal of Applied Earth Observation and Geoinformation, 23, 301-312.

Arthur D., Vassilvitskii S. 2007 Proc. Eighteenth Annual ACM-SIAM Symp. on Discrete Algorithms SODA '07 (Philadelphia, PA: SIAM) 1027

Atzberger, C., 2013. Advances in remote sensing of agriculture: Context description, existing operational monitoring systems and major information needs. Remote sensing, 5(2), pp.949-981.

Bargoti, S. and Underwood, J., 2017, May. Deep fruit detection in orchards. In 2017 IEEE international conference on robotics and automation (ICRA) (pp. 3626-3633). IEEE.

Basso, B., Fiorentino, C., Cammarano, D., Schulthess, U., 2016. Variable rate nitrogen fertilizer response in wheat using remote sensing. Precision agriculture, 17, pp.168-182.

Claverie, E., Meunier, F., Javaux, M., Sadok, W., 2018. Increased contribution of wheat nocturnal transpiration to daily water use under drought. Physiologia Plantarum, 162(3), pp.290-300.

Didan, K., Munoz, A. B., Solano, R., Huete, A., 2015. MODIS vegetation index user's guide (MOD13 series). University of Arizona: Vegetation Index and Phenology Lab, 35, 2-33.

Delbart, N., Kergoat, L., Le Toan, T., Lhermitte, J., Picard, G., 2005. Determination of phenological dates in boreal regions using normalized difference water index. Remote Sensing of Environment, 97(1), pp.26-38.

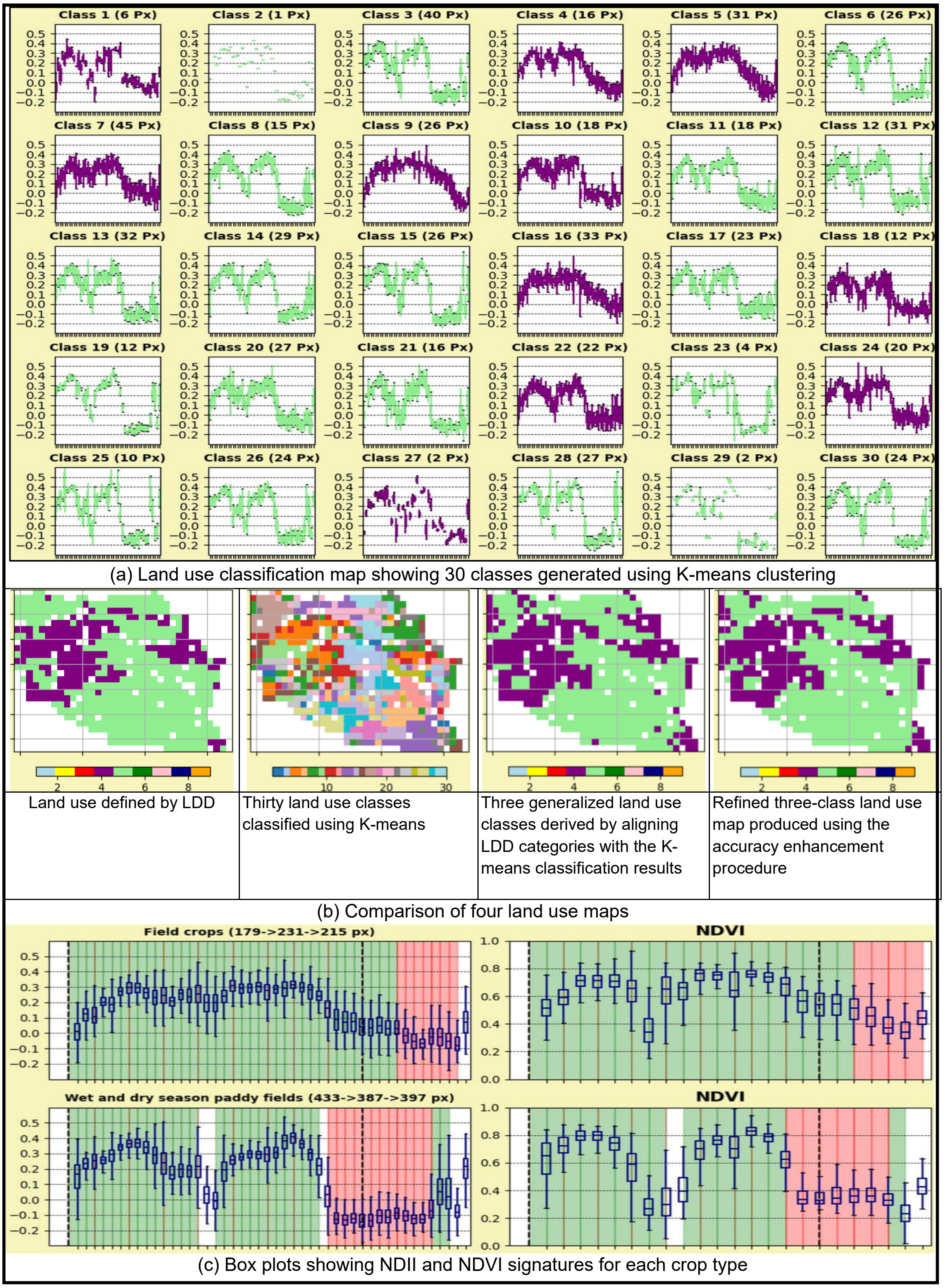

Figure 2. NDII-based land use classification for Kraseaw Irrigation Project in 2017

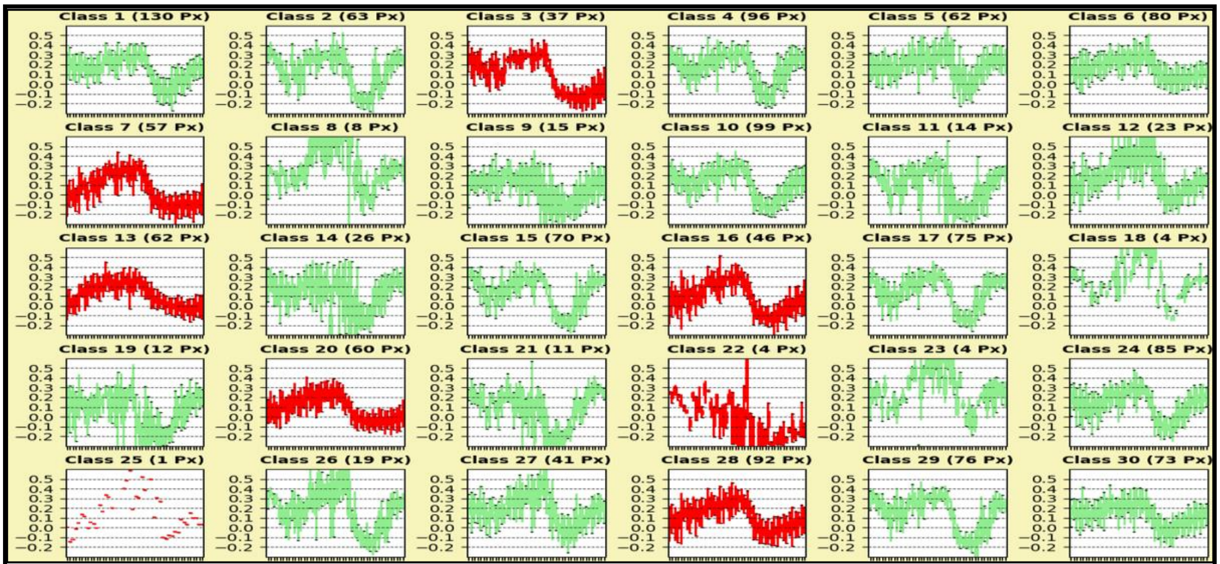

(a) Land use classification map showing 30 classes generated using K-means clustering

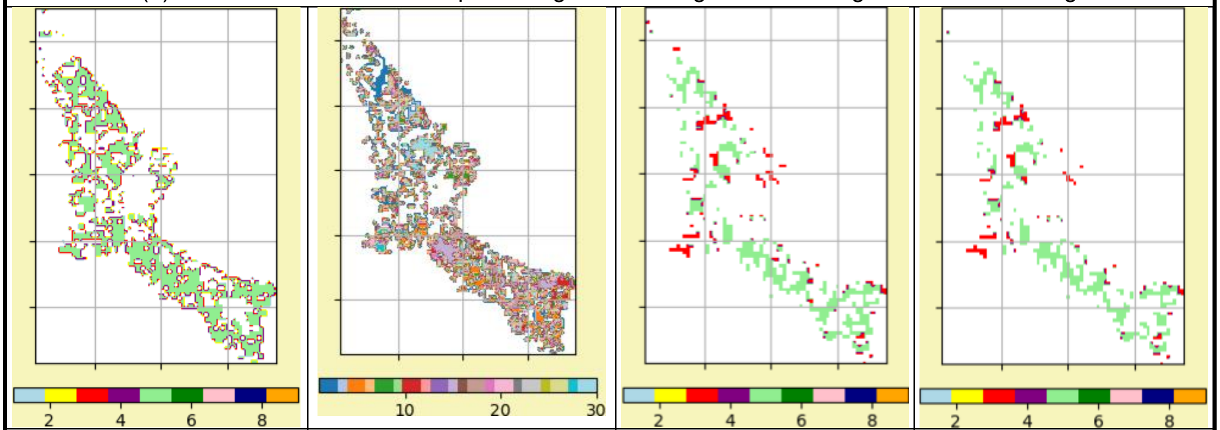

Land use defined by LDD	Thirty land use classes classified using K-means	Three generalized land use classes derived by aligning LDD categories with the K-means classification results	Refined three-class land use map produced using the accuracy enhancement procedure

(b) Comparison of four land use maps

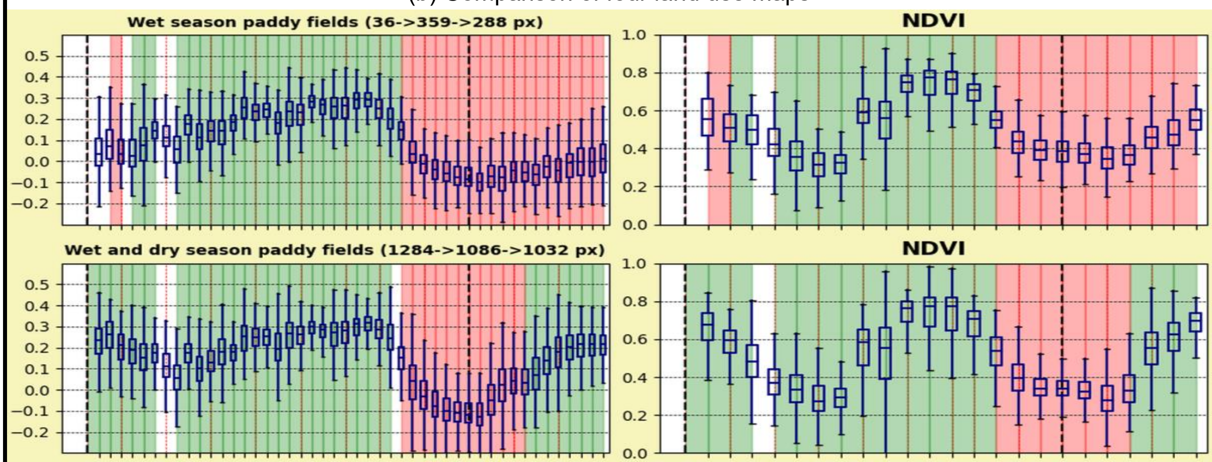

(c) Box plots showing NDII and NDVI signatures for each crop type

Figure 3. NDII-based land use classification for Nongwai Irrigation Project in 2017

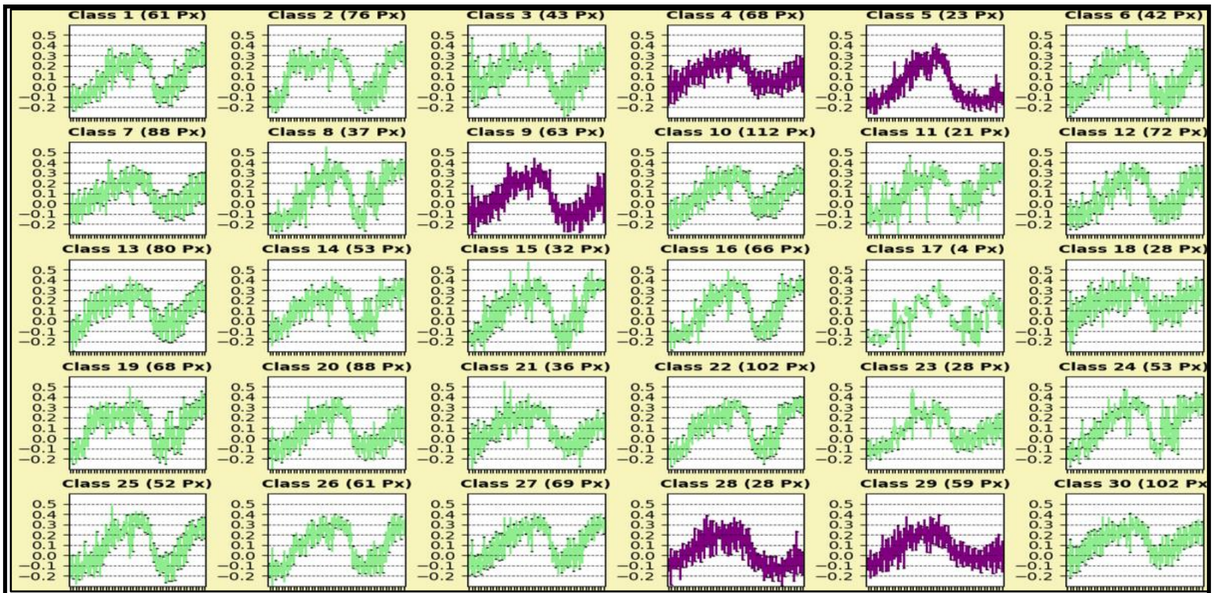

(a) Land use classification map showing 30 classes generated using K-means clustering

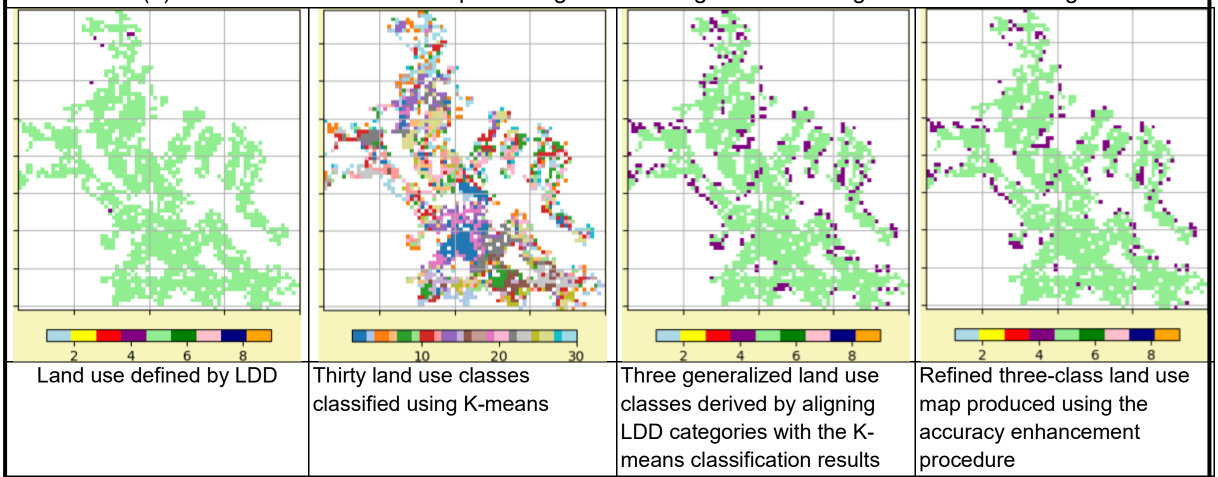

(b) Comparison of four land use maps

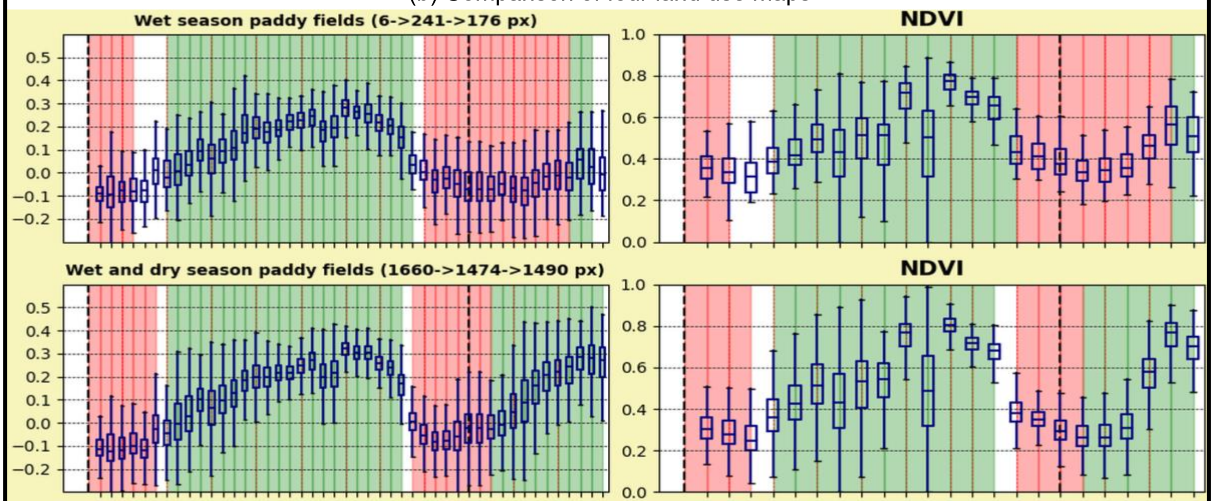

(c) Box plots showing NDII and NDVI signatures for each crop type

Figure 4. NDII-based land use classification for Lampao Irrigation Project in 2013

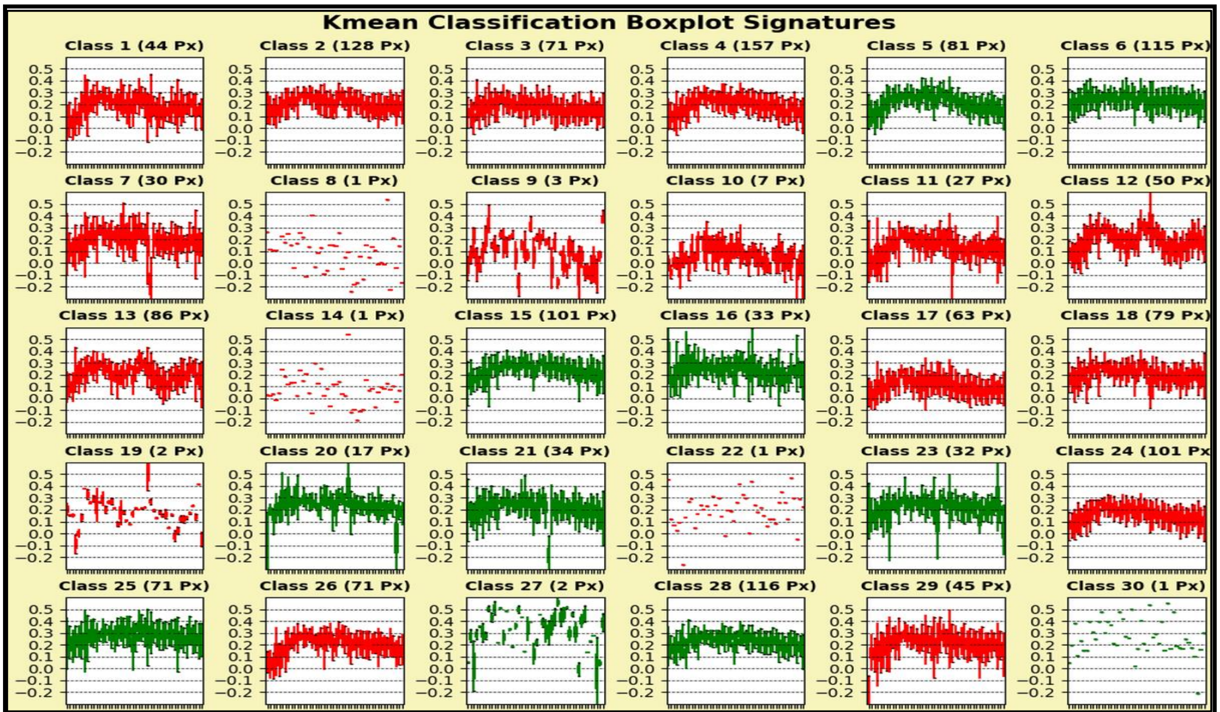

(a) Land use classification map showing 30 classes generated using K-means clustering

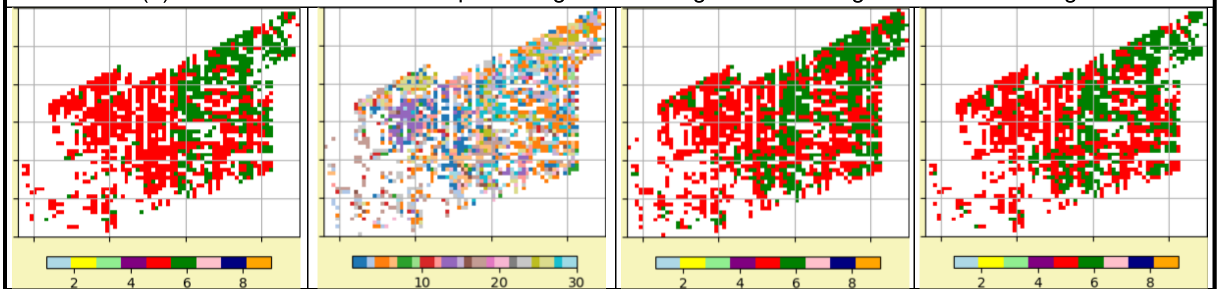

Land use defined by LDD	Thirty land use classes classified using K-means	Three generalized land use classes derived by aligning LDD categories with the K-means classification results	Refined three-class land use map produced using the accuracy enhancement procedure

(b) Comparison of four land use maps

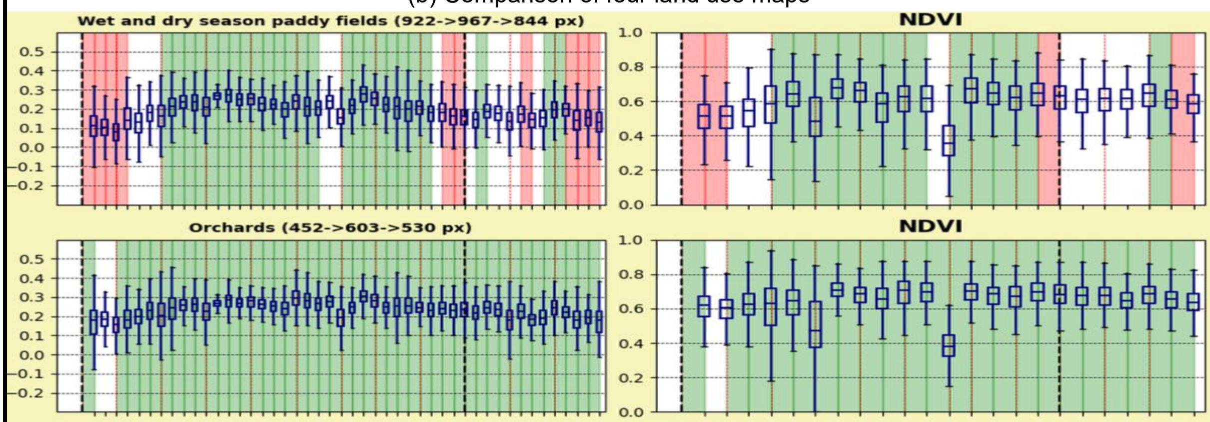

(c) Box plots showing NDII and NDVI signatures for each crop type

Figure 5. NDII-based land use classification for Northern Rangsit Irrigation Project in 2017

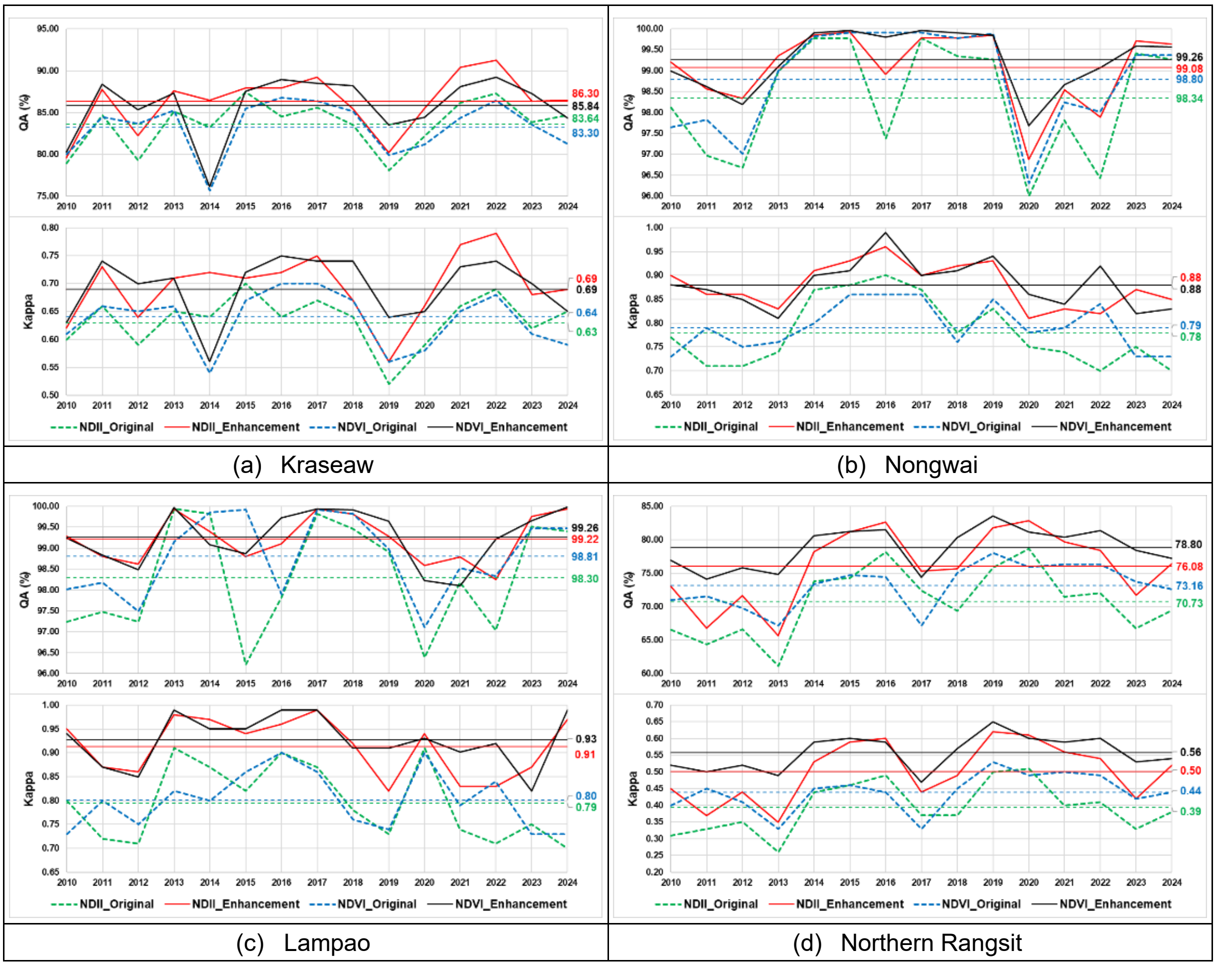

Figure 6. Comparison of original and enhanced Overall Accuracy (OA) and Kappa Coefficient (K) in land use classification across four irrigation projects (2013-2024)

Dorj, U.O., Lee, M., Yun, S.S., 2017. An yield estimation in citrus orchards via fruit detection and counting using image processing. Computers and electronics in agriculture, 140, pp.103-112.

Duveiller, G., Defourny, P., 2010. A conceptual framework to define the spatial resolution requirements for agricultural monitoring using remote sensing. Remote Sensing of Environment, 114(11), pp.2637-2650.

Eisfelder, C., Asam, S., Hirner, A., Reiners, P., Holzwarth, S., Bachmann, M., Gessner, U., Dietz, A., Huth, J., Bachofer, F., 2023. Seasonal Vegetation Trends for Europe over 30 Years from a Novel Normalised Difference Vegetation Index (NDVI) Time-Series—The TIMELINE NDVI Product. Remote Sensing, 15(14), 3616.

Gao, B., 1996. NDWI - A normalized difference water index for remote sensing of vegetation liquid water from space. Remote Sensing of Environment 58, 257-266.

Gonsamo, A., Chen, J.M., Price, D.T., Kurz, W.A. and Wu, C., 2012. Land surface phenology from optical satellite measurement and CO2 eddy covariance technique. Journal of Geophysical Research: Biogeosciences, 117(G3).

Hardisky, M.A., Klemas, V., Smart, R.M., 1983. The influence of soil-salinity, growth form, and leaf moisture on the spectral radiance of Spartina alterniflora canopies. Photogrammetric Engineering and Remote Sensing 49, 77-83.

Hatfield, J.L., Prueger, J.H., 2010. Value of using different vegetative indices to quantify agricultural crop characteristics at different growth stages under varying management practices. Remote Sensing, 2(2), pp.562-578.

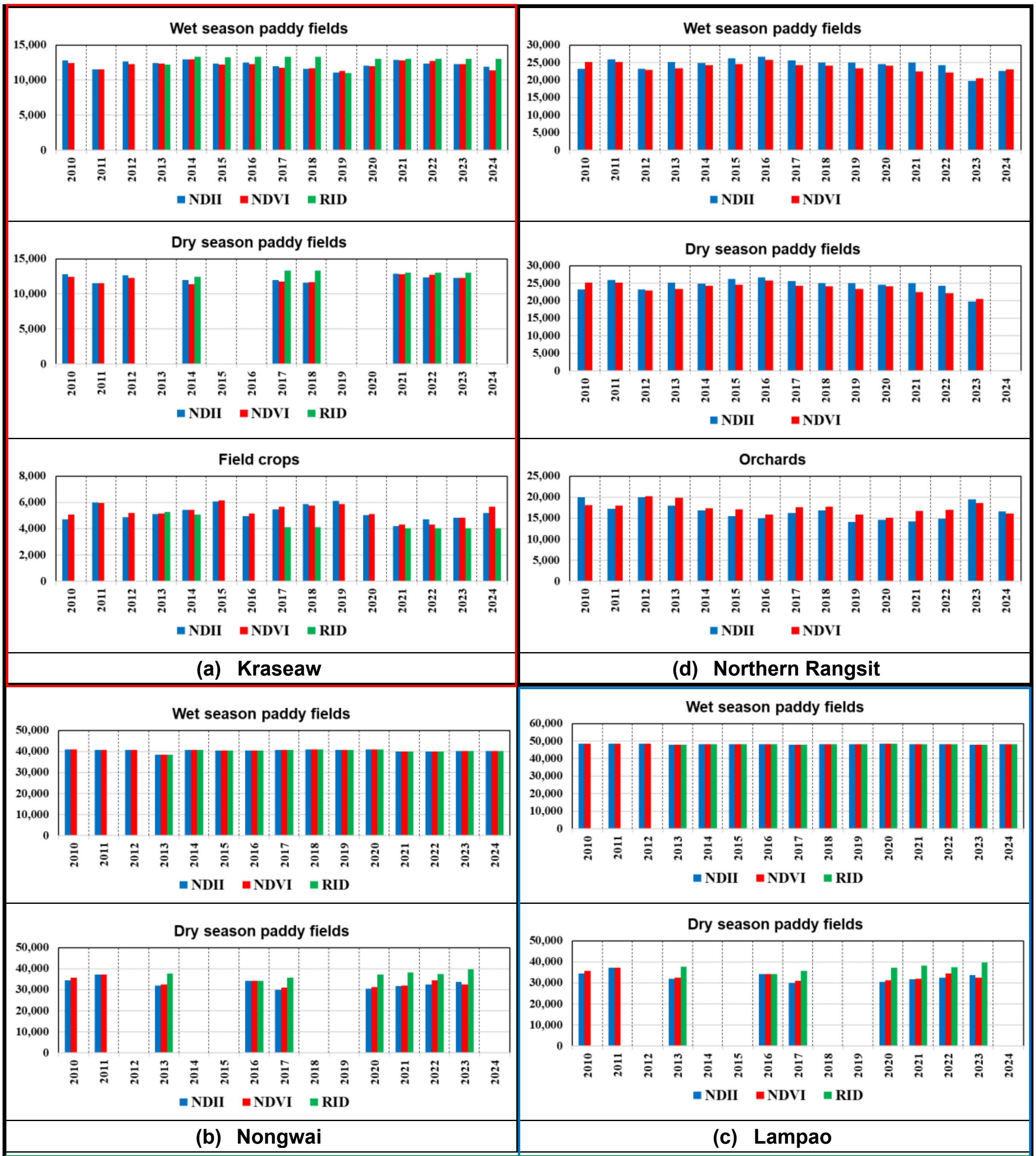

Project	Relative RMSE (%)			R^2		
	NDII-NDVI	NDII-RID	NDVI-RID	NDII-NDVI	NDII-RID	NDVI-RID
Kraseaw	2.00	7.68	8.34	1.00	0.97	0.97
Nongwai	1.42	7.67	7.18	0.99	0.74	0.72
Lampao	2.15	3.81	4.54	0.90	0.70	0.61
Northern Rangsit	6.89	-	-	0.95	-	-

Figure 7. Comparison of crop areas classified using NDVI and NDII with reported irrigated areas from RID across four irrigation projects (2010-2024)

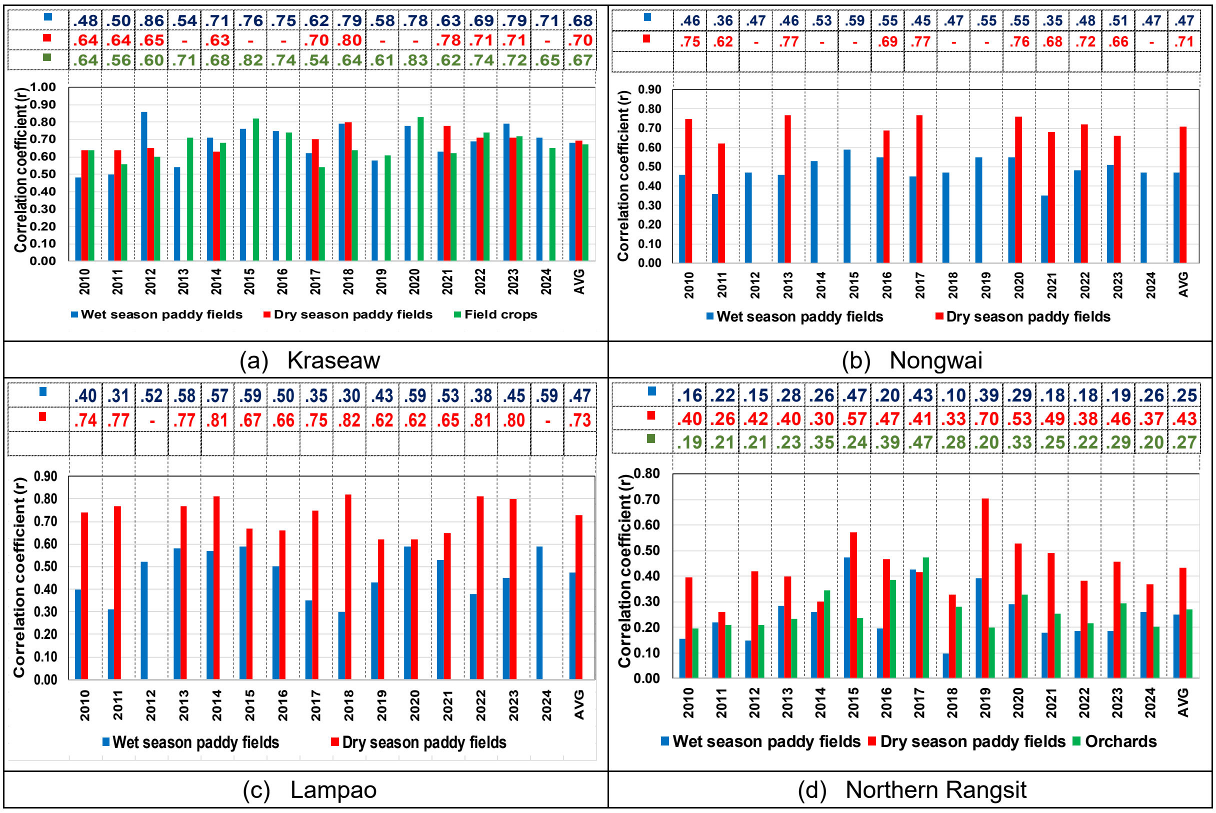

Figure 8. Comparison of correlation coefficient (r) between NDII and NDVI for different crops across four irrigation projects (2013-2024)

Liu, Y., Engel, B.A., Flanagan, D.C., Gitau, M.W., McMillan, S.K., Chaubey, I., 2017. A review on effectiveness of best management practices in improving hydrology and water quality: Needs and opportunities. Science of the Total Environment, 601, pp.580-593.

Liu, S., Wang, Y., Zhang, G. J., Wei, L., Wang, B., Yu, L., 2022. Contrasting influences of biogeophysical and biogeochemical impacts of historical land use on global economic inequality. Nature Communications, 13(1), 2479.

Lloyd, S. (1982). Least squares quantization in PCM. IEEE transactions on information theory, 28(2), 129-137.

Lobell, D.B., Thau, D., Seifert, C., Engle, E., Little, B., 2015. A scalable satellite-based crop yield mapper. Remote Sensing of Environment, 164, pp.324-333.

Lu, D. and Weng, Q., 2007. A survey of image classification methods and techniques for improving classification performance. International journal of Remote sensing, 28(5), pp.823-870.

Mulla, D.J., 2013. Twenty five years of remote sensing in precision agriculture: Key advances and remaining knowledge gaps. Biosystems engineering, 114(4), pp.358-371.

Olofsson, P., Foody, G.M., Stehman, S.V. and Woodcock, C.E., 2013. Making better use of accuracy data in land change studies: Estimating accuracy and area and quantifying uncertainty using stratified estimation. Remote sensing of environment, 129, pp.122-131.

Peters, A.J., Walter-Shea, E.A., Ji, L., Vina, A., Hayes, M. and Svoboda, M.D., 2002. Drought monitoring with NDVI-based standardized vegetation index. Photogrammetric engineering and remote sensing, 68(1), pp.71-75.

Pickering, J., Tyukavina, A., Khan, A., Potapov, P., Adusei, B., Hansen, M.C. and Lima, A., 2021. Using multi-resolution satellite data to quantify land dynamics: Applications of PlanetScope imagery for cropland and tree-cover loss area estimation. Remote Sensing, 13(11), p.2191.

Rogan, J. and Chen, D., 2004. Remote sensing technology for mapping and monitoring land-cover and land-use change. Progress in planning, 61(4), pp.301-325.

Rouse, J.W., Hass, R.H., Schell, J.A., Deering, D.W., 1973. Monitoring vegetation systems in the Great Plains with ERTS. Third ERTS Symposium, NASA SP-351 I, 309-317.

Serrano, L., Filella, I., Penuelas, J., 2000. Remote sensing of biomass and yield of winter wheat under different nitrogen supplies. Crop science, 40(3), pp.723-731.

Sharma, M., Kumar, C.J., Deka, A., 2021. Land cover classification: a comparative analysis of clustering techniques using Sentinel-2 data. International Journal of Sustainable Agricultural Management and Informatics, 7(4), pp.321-342.

Sharma, G., Sharma, L., Sharma, K., 2019. Assessment of land use change and its effect on soil carbon stock using multitemporal satellite data in semiarid region of Rajasthan, India. Ecological Processes, 8, 1-17.

Sishodia, R.P., Ray, R.L., Singh, S.K., 2020. Applications of remote sensing in precision agriculture: A review. Remote sensing, 12(19), p.3136.

Steele-Dunne, S. C., Friesen, J., Van De Giesen, N., 2012. Using diurnal variation in backscatter to detect vegetation water stress. IEEE Transactions on Geoscience and Remote Sensing, 50(7), 2618-2629.

Thenkabail, P.S., Knox, J.W., Ozdogan, M., Gumma, M.K., Congalton, R.G., Wu, Z., Milesi, C., Finkral, A., Marshall, M., Mariotto, I., You, S., 2012. Assessing future risks to agricultural productivity, water resources and food security: How can remote sensing help?. Photogrammetric Engineering & Remote Sensing, 78(8).

Tucker, C.J., 1979. Red and photographic infrared linear combinations for monitoring vegetation. Remote sensing of Environment, 8(2), pp.127-150.

Vermote, E., 2015. MOD09A1 MODIS/terra surface reflectance 8-day L3 global 500m SIN grid V006. NASA EOSDIS Land Processes DAAC, 10.

Wang, Q., Tenhunen, J. D., 2004. Vegetation mapping with multitemporal NDVI in North Eastern China transect (NECT). International Journal of Applied Earth Observation and Geoinformation, 6(1), 17-31.

Wardlow, B.D., Egbert, S.L., 2008. Large-area crop mapping using time-series MODIS 250 m NDVI data: An assessment for the US Central Great Plains. Remote sensing of environment, 112(3), pp.1096-1116.

Zhang, X., Friedl, M.A., Schaaf, C.B., Strahler, A.H., Hodges, J.C., Gao, F., Reed, B.C. and Huete, A., 2003. Monitoring vegetation phenology using MODIS. Remote sensing of environment, 84(3), pp.471-475.

Zhao, J., Dong, Y., Zhang, M., Huang, L., 2020. Comparison of identifying land cover tempo-spatial changes using GlobCover and MCD12Q1 global land cover products. Arabian Journal of Geosciences, 13, pp.1-12.